Defence Research and Development Canada
Recherche et développement pour la défense Canada

DEFENCE R&D DÉFENSE

A design optimization framework for multi-band body-of-revolution antenna feeds

Application to a prime-focus dual-band Ku/X coaxial feed

Éric Choinière and Gilbert A. Morin

Defence R&D Canada – Ottawa
TECHNICAL MEMORANDUM
DRDC Ottawa TM 2005-216
December 2005

Canada

A design optimization framework for multi-band body-of-revolution antenna feeds

Application to a prime-focus dual-band Ku/X coaxial feed

Éric Choinière

Gilbert A. Morin

Defence R&D Canada – Ottawa

Technical Memorandum

DRDC Ottawa TM 2005-216

December 2005

Author

Original signed by Éric Choinière

Éric Choinière

Approved by

Original signed by Bill Katsube

Bill Katsube
Head/CNEW Section

Approved for release by

Original signed by Anthony Ashley

Anthony Ashley
Head/Document Review Panel

Abstract

The development of software radios has brought about a need for multi-band antenna feeds for use in the radio-frequency front-ends of satellite ground terminals. To provide the tools necessary for the design of such feeds, we have developed the *Framework for Antenna Design and Optimization* (FADO), a computer-based antenna design optimization framework based on the combination of custom-designed synthesis and analysis software, a commercial body-of-revolution electromagnetics simulation tool (AKBOR2, by Kishk Consulting), a high-frequency reflector modelling tool (Grasp, by TICRA), and a global optimizer (*glbfast*, part of the Tomlab optimization suite). The capabilities of this new design tool are demonstrated through the design of a compact dual-band Ku/X coaxial antenna feed for a 4.6-m single-reflector antenna.

A compact dual-band feed was designed by combining a dielectric-filled circular waveguide ending in a tapered dielectric rod, which launches the Ku-band waves, and a coaxial aperture launching the X-band waves. The use of a high dielectric constant material ($\epsilon_r = 9.8$) within the Ku-band's circular waveguide resulted in a fairly compact dual-band feed design aperture with an outer diameter of 2.8 cm.

Directly integrating both the feed scattering parameters and the secondary beam characteristics within a global optimization loop, this dual-band Ku/X coaxial antenna feed was designed and optimized using FADO. Proper reflector illumination was achieved in both frequency bands. This resulted in aperture efficiencies above 67% at X band and 59% at Ku band, secondary-beam cross-polarization levels of -57 dB at X band and -37 dB at Ku band, and sidelobe levels lower than the maximum sidelobe envelope per IntelSat's standard. A ring-based filter integrated in the coaxial channel is shown to improve coaxial rejection of the Ku-band signal while providing adequate impedance matching capability for the X-band signal. A Ku-band isolation better than -19.3 dB and an X-band input mismatch better than -17 dB are achieved. Further improvements in the channel isolation may be achieved using additional coaxial rings in the coaxial waveguide.

As part of a separate optimization, two air gap rings were integrated within the dielectric-filled circular waveguide, which allowed for an improvement of the Ku-band input mismatch from -10.5 dB to -16.2 dB.

The capabilities of FADO will allow for the efficient synthesis and optimization of multi-band antenna feeds integrated in symmetrically-fed single reflector antennas. In addition, straightforward extensions of the design framework could allow for the synthesis and optimization of dual-reflector, and/or offset-fed antenna systems. Finally, FADO may be extended for use with other antenna simulation tools, to address other classes of antenna geometries which may not be rotationally symmetric.

Résumé

Le développement des radios logicielles a engendré de nouveaux besoins en matière d'antennes sources pour utilisation dans les étages d'entrée radio-fréquence des terminaux terrestres de communications par satellite. Afin de permettre la conception de telles antennes sources, nous avons développé le *cadriciel de conception et d'optimisation d'antennes*(FADO)[1], un cadriciel d'optimisation de géométrie d'antenne combinant des éléments logiciels maison de synthèse et d'analyse, un outil commercial de simulation électromagnétique de corps à symétrie de révolution (AKBOR2, de Kishk Consulting), un outil de modélisation haute fréquence pour réflecteurs (Grasp, de TICRA) et un optimisateur global (*glbfast*, un élément de la suite logicielle Tomlab). Le potentiel de ce nouvel outil de conception est démontré dans le cadre de la conception d'une antenne source coaxiale compacte à deux bandes Ku/X devant être intégré à une antenne à simple réflecteur de 4,6 m.

Une antenne source compacte à deux bandes est réalisée en combinant un guide d'ondes circulaire rempli d'un matériau diélectrique et se terminant en une excroissance profilée du matériau diélectrique de laquelle émanent les ondes en bande Ku, ainsi qu'une ouverture coaxiale d'où rayonnent les ondes en bande X. L'utilisation d'un matériau de constante diélectrique élevée ($\epsilon_r = 9,8$) à l'intérieur du guide circulaire permet la réalisation d'une ouverture à deux bandes relativement compacte, ayant un diamètre extérieur de 2,8 cm.

Intégrant directement à la fois les coefficients de dispersion et les caractéristiques du faisceau secondaire à l'intérieur d'une boucle d'optimisation globale, une antenne source coaxiale à deux bandes Ku/X est conçue et optimisée à l'aide de FADO. Une illumination adéquate du réflecteur est obtenue dans les deux bandes de fréquence. Les résultats indiquent des efficacités d'ouverture supérieures à 67% dans la bande X et 59% dans la bande Ku, des niveaux de polarisation croisée du faisceau secondaire de -57 dB dans la bande X et de -37 dB dans la bande Ku, et des niveaux de lobes secondaires inférieurs à l'enveloppe maximale prescrite selon le standard d'IntelSat. Un filtre à base d'anneaux métalliques, intégré dans le guide d'ondes coaxial, permet d'améliorer la réjection du signal Ku tout en permettant l'adaptation adéquate de l'impédance d'entrée en bande X. Ainsi, l'isolation en bande Ku est de $-19,3$ dB et la désadaptation d'impédance à l'entrée du guide coaxial en bande X est de -17 dB. Des améliorations subséquentes de l'isolation pourraient être réalisées par l'ajout d'anneaux supplémentaires dans le guide coaxial.

Lors d'une optimisation additionnelle, deux anneaux d'air ont été intégrés à l'intérieur du guide d'ondes circulaire rempli d'un matériau diélectrique, permettant une réduction de la désadaptation d'impédance d'entrée en bande Ku de $-10,5$ dB à $-16,2$ dB.

FADO permet la synthèse et l'optimisation efficaces d'antennes source intégrées à des antennes à simple réflecteur à alimentation symétrique. De plus, de simples extensions du cadriciel pourraient permettre la synthèse et l'optimisation d'antennes à double réflecteur et/ou d'antennes à alimentation excentrée.

[1] En Anglais : *Framework for Antenna Design and Optimization.*

Executive summary

A design optimization framework for multi-band body-of-revolution antenna feeds: Application to a prime-focus dual-band Ku/X coaxial feed

Éric Choinière, Gilbert A. Morin; DRDC Ottawa TM 2005-216; Defence R&D Canada – Ottawa; December 2005.

Background

The development of software radios and their application to military satellite communications has brought about a need for multi-band-capable satellite ground terminals. Enabling multi-band capabilities can be accomplished through the retrofitting of existing prime-focus reflector antennas with newly designed multi-band antenna feeds.

To provide the software tools necessary for the design of such multi-band feeds, we have developed the *Framework for Antenna Design and Optimization* (FADO), a computer-based antenna design optimization framework based on the combination of four primary components:

- custom-designed antenna synthesis and analysis software;
- a commercial body-of-revolution electromagnetic simulation tool (AKBOR2, by Kishk Consulting);
- a high-frequency reflector modelling tool (Grasp, by TICRA);and
- an industrial global optimizer (*glbfast*, from the Tomlab optimization suite).

The capabilities of this new design tool are demonstrated through the design of a compact dual-band coaxial antenna feed supporting the Ku and X bands, adapted to a 4.6-m-diameter prime-focus reflector antenna.

Principal Results

The design of a dual-band coaxial Ku/X feed using FADO has shown that this new antenna design optimization framework is an efficient tool that will enable future designs of novel multi-band feeds relevant to the Canadian Forces' future needs in multi-band satellite communications. The ability to directly account for the secondary beam characteristics (the beam generated by the reflector and aimed at the satellite) within the optimization loop, as opposed to optimizing the feed based on its primary radiation characteristics, is key to finding the best possible feed design for a given reflector geometry.

A compact dual-band feed was designed by combining a dielectric-filled circular waveguide ending in a tapered dielectric rod and carrying the Ku-band signal, and a coaxial waveguide

aperture radiating the X-band signal. The use of a high-constant dielectric ($\epsilon_r = 9.8$) within the Ku-band's circular waveguide resulted in a fairly compact dual-band feed aperture with an outer diameter of 2.8 cm. Proper reflector illumination was achieved in both frequency bands. This resulted in aperture efficiencies above 67% at X band and 59% at Ku band, secondary-beam cross-polarization levels of -57 dB at X band and -37 dB at Ku band, and sidelobe levels lower than the maximum sidelobe envelope per IntelSat's standard.

One of the main concerns in such coaxial structures is the penetration of the higher frequency signal (here, the Ku-band signal) into the lower-frequency channel (here, the X-band coaxial channel). This issue was successfully mitigated by blocking the Ku-band signal in the coaxial channel using a low-pass filter implemented with a series of three metallic rings inserted in the coaxial waveguide. An isolation of -19.3 dB was achieved, while at the same time providing an acceptable input impedance mismatch of -17 dB at X band.

In an independent optimization, improvements in the Ku-band input impedance match were obtained with the integration of two air gap rings within the dielectric-filled circular waveguide. This has resulted in a reduction of the input impedance mismatch from -10.5 dB to -16.2 dB.

Significance of Results

The capabilities of FADO allow for the efficient synthesis and optimization of the radiating stage of a multi-band antenna feed integrated in a symmetrically-fed single reflector antenna. This new tool, combined with other ongoing efforts to develop other feed components connecting upstream of the radiating stage developed here, will provide DRDC with the capability to develop new custom-designed multi-band antenna feeds to retrofit the Canadian Forces' existing single-band satellite terminals and effectively upgrade them for multi-band operation.

Future Work

Straightforward extensions of the design framework shown here could allow for the synthesis and optimization of dual-reflector, and/or offset-fed antenna systems. In addition, FADO may be extended for use with other antenna simulation tools, allowing to address other classes of antenna geometries which may not be rotationally symmetric.

Other ongoing research efforts also focus on the development of the other feed components, which connect upstream of the radiating stage. These include polarizers, orthomode transducers, and coaxial waveguide couplers.

Sommaire

A design optimization framework for multi-band body-of-revolution antenna feeds: Application to a prime-focus dual-band Ku/X coaxial feed

Éric Choinière, Gilbert A. Morin; DRDC Ottawa TM 2005-216; R & D pour la défense Canada – Ottawa; décembre 2005.

Contexte

Le développement des radios logicielles et leur application aux communications militaires par satellite a créé une demande de terminaux terrestres ayant des fonctions multibandes. Ces capacités multibandes peuvent être obtenues par la mise à niveau d'antennes à simple réflecteur existantes au moyen de nouvelles antennes source multibandes.

Afin de disposer d'outils logiciels nécessaire à la conception de telles antennes sources multibandes, nous avons développé le *cadriciel de conception et d'optimisation d'antennes* (FADO)[2], un cadriciel d'optimisation de géométrie d'antenne combinant 4 composantes principales :
– des éléments de synthèse et d'analyse développés sur mesure ;
– un outil commercial de simulation électromagnétique de corps à symétrie de révolution (AKBOR2, de Kishk Consulting) ;
– un outil de modélisation haute fréquence pour réflecteurs (Grasp, de TICRA) ; et
– un optimisateur global (*glbfast*, de la suite logicielle d'optimisation Tomlab).
Le potentiel de ce nouvel outil de conception est démontré par la conception d'une antenne source coaxiale compacte à deux bandes supportant les bandes Ku et X, adaptée à une antenne à simple réflecteur d'un diamètre de 4,6 m.

Résultats Principaux

La conception d'une antenne source coaxiale Ku/X à l'aide de FADO a permis de démontrer que ce nouveau cadriciel d'optimisation de géométrie d'antenne est un outil efficace qui permettra la conception future de nouvelles antennes source multibandes applicables aux besoins futurs des Forces Canadiennes en matière de communications multibandes par satellite. La possibilité de prendre en compte directement des caractéristiques du faisceau secondaire (le faisceau produit par le réflecteur et dirigé vers le satellite) à l'intérieur de la boucle d'optimisation, plutôt que d'optimiser une antenne source à partir de ses caractéristiques de rayonnement primaire, est un élément clé dans la recherche de la géométrie optimale d'une antenne source pour une géométrie de réflecteur donnée.

Une antenne source compacte à deux bandes est réalisée en combinant un guide d'ondes circulaire rempli de matériau diélectrique et se terminant en une excroissance profilée du

[2]En Anglais : *Framework for Antenna Design and Optimization.*

matériau diélectrique de laquelle émanent les ondes en bande Ku, ainsi qu'une ouverture coaxiale d'où rayonnent les ondes en bande X. L'utilisation d'un matériau de constante diélectrique élevée ($\epsilon_r = 9,8$) à l'intérieur du guide circulaire permet la réalisation d'une ouverture à deux bandes relativement compacte, ayant un diamètre extérieur de 2,8 cm. Une illumination adéquate du réflecteur est accomplie dans les deux bandes de fréquence, avec pour résultat des efficacités d'ouverture supérieures à 67% dans la bande X et 59% dans la bande Ku, des niveaux de polarisation croisée du faisceau secondaire de -57 dB dans la bande X et de -37 dB dans la bande Ku, et des niveaux de lobes secondaires inférieurs à l'enveloppe maximale prescrite selon le standard d'IntelSat.

L'une des inquiétudes principales dans de telles structures coaxiales est la pénétration du signal haute fréquence (ici, le signal Ku) dans le canal destiné à la basse fréquence (ici, le canal coaxial destiné à la bande X). Pour pallier à ce problème, un filtre passe-bas, réalisé au moyen d'une série de trois anneaux métalliques, a été intégré à l'intérieur du canal coaxial. Une isolation de $-19,3$ dB a ainsi été atteinte, tout en obtenant un niveau acceptable de désadaptation d'impédance d'entrée en bande X, soit -17 dB.

Lors d'une optimisation additionnelle, une amélioration de l'adaptation d'impédance d'entrée en bande Ku a été obtenue au moyen de l'intégration de deux anneaux d'air à l'intérieur du guide d'ondes circulaire rempli d'un matériau diélectrique. Cette modification a permis d'obtenir une réduction de la désadaptation d'impédance d'entrée de $-10,5$ dB à $-16,2$ dB.

Portée des Résultats

FADO permet la synthèse et l'optimisation efficaces de l'étage rayonnant d'une antenne source multibandes intégrée à une antenne à simple réflecteur à alimentation symétrique. Ce nouvel outil, combiné à d'autres efforts de recherche portant sur les composantes se rattachant en amont de l'étage rayonnant, fournira à RDDC la capacité de développer de nouvelles antennes source multibandes pour adapter les terminaux terrestres mono-bande de communications satellite présentement utilisés par les Forces Canadiennes.

Perspectives

De simples extensions du cadriciel présenté ici pourraient permettre la synthèse et l'optimisation de systèmes à deux réflecteurs et/ou à alimentation excentrée. De plus, les capacités de FADO pourraient être étendues de façon à permettre l'intégration d'autres outils de simulation d'antennes, ouvrant ainsi la possibilité d'étudier d'autres classes de géométries d'antennes source ne présentant pas une symétrie de révolution.

D'autres efforts de recherche en cours se concentrent sur le développement des autres composantes de l'antenne source se rattachant en amont de l'étage rayonnant. Parmi celles-ci, on compte les polariseurs, les transducteurs orthomodes et les coupleurs de guide d'ondes coaxial.

Table of contents

List of figures

List of tables

1 Introduction

The development of software radios and their application to military satellite communications has brought about a need for multi-band-capable satellite ground terminals. Enabling multi-band capabilities can be accomplished through the retrofitting of existing prime-focus reflector antennas with newly designed multi-band antenna feeds.

To provide the software tools necessary for the design of such multi-band feeds, we have developed the *Framework for Antenna Design and Optimization* (FADO), which combines custom-designed antenna synthesis and analysis software and the commercial antenna simulation packages AKBOR2 [1] and Grasp [2].

This document presents this new optimization framework along with the theory and methods used in the custom-designed software that are part of it. In addition, the capabilities of this new design tool are demonstrated through the design of a compact dual-band coaxial antenna feed supporting the Ku and X bands, adapted to a 4.6-m-diameter prime-focus reflector antenna. Note that the reflector's focal point is such that $f/D = 0.33$, where f is the distance from the apex to the focal point and D is the reflector diameter.

A tri-band antenna is ultimately sought for the RF front-end of a demonstration satellite terminal providing coverage in the C, X and Ku bands. A future demonstration platform would be designed to operate in the Ku and C bands supported by Anik F2 (see specifications online [3]), as identified in Table 1, and in the X band for military use. An internal report provides more detail on the specifications of interest [4].

As an intermediate step, however, a preliminary dual-band design supporting the Ku and X bands is first considered and is used throughout this report to demonstrate the capabilities offered by FADO. Note that the design and optimization strategy presented here appear to bear some similarities with the approach used in the design of a Ka/X dual-band feed presented in [5].

In section 2, we present an overview of the antenna design optimization framework devised and implemented as part of this work. Section 3 presents the AKBOR2 full-wave simulation tool for bodies of revolution, briefly describes improvements for numerical stability, and presents the in-house synthesis and analysis capabilities. Section 4 describes the high-frequency analysis of reflector performance. Section 5 defines the single-valued scalar cost

Frequency Band	Tx Band	Rx Band
C — Anik F2	5.925 to 6.425 GHz	3.700 to 4.200 GHz
X — Military	**7.90 to 8.40 GHz**	**7.25 to 7.75 GHz**
Ku — Anik F2	**14.0 to 14.5 GHz**	**11.70 to 12.20 GHz**

Table 1: *Frequency Bands under consideration for a Tri-band Satellite Terminal Compatible with Anik F2 in the C and Ku frequency bands. The frequency bands shown in bold format are supported by the dual-band Ku/X feed developed as part of this report.*

function, based on various antenna performance criteria, that is used for design optimization purposes. Section 6 details the two-stage procedure followed to optimize our dual-band Ku/X feed design. Finally, section 7 concludes this report.

2 Antenna Design Optimization Framework

2.1 Overview

A combination of commercial software tools and custom-designed software was employed to assemble an optimization framework suitable for rotationally-symmetric antenna feeds (bodies of revolution). The data flow diagram shown in Figure 1 maps out the roles of various software components within the antenna analysis and optimization framework.

The general aim is to optimize an objective cost based on antenna performance and desired goals. Matlab [6] is used as the main computing environment for the optimization framework. Custom-designed Matlab routines provide the necessary links for connectivity among the various software components. These routines, along with commercial simulation software tools AKBOR2 [1] and Grasp [2], are used to implement a "cost function" used by the optimizer (Tomlab's *glbfast*) [7].

2.2 Global Optimizer

The cost function that we are trying to minimize is a single-valued function of several variables, the design parameters. Generally speaking, the cost function obtained as a result of the evaluation of the antenna's performance is not expected to be a convex function. Since most classical optimization algorithms use gradient (or Jacobian) information to minimize the objective function, they tend to converge to the function's nearest local minimum and are therefore of little use in obtaining a global minimum corresponding to the optimal antenna for a given set of design parameters.

Several alternative approaches to optimization exist which do not rely on the use of gradients, and are therefore more suitable for finding a global minimum. We note that this global searching capability, however, does come at a cost: global optimizers are not nearly as efficient as gradient optimizers in finding the minimum of a convex function. Thus, wherever an objective function is known to be convex, or can be constrained to be convex, gradient optimizers should be favoured.

Since this is not the case here, we have chosen to use the *Direct* [8] algorithm for our global optimization. *Direct* is a global optimization algorithm for minimizing a multivariate function subject to lower and upper bounds on the variables. It uses a space-partitioning approach to identify the basin of convergence of the optimum and a local search to exploit it. Its key characteristic is that it performs both the global and local searches simultaneously.

As indicated in Figure 1, we have chosen to use Tomlab's *glbfast* global solver which implements the *Direct* algorithm. This solver was part of the Tomlab base module purchased

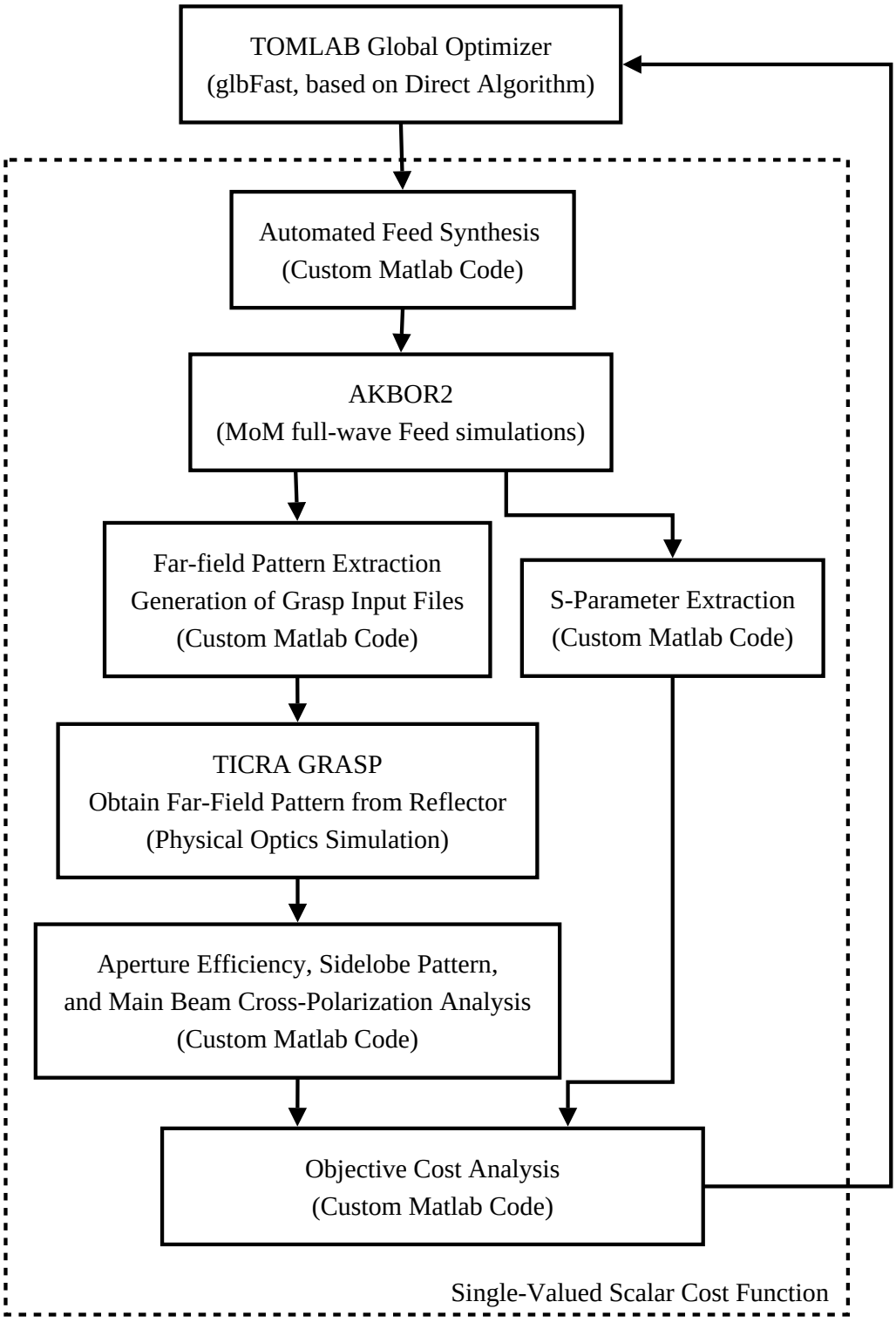

Figure 1: *Data flow diagram of the* Framework for Antenna Design and Optimization.

from Tomlab Optimization Inc.

Alternative global optimization schemes could be tested in the future, such as Tomlab's rbfsolve (Radial Basis Function interpolation algorithm) or ego (Efficient Global Optimization) algorithms, both of which are specifically designed for costly objective functions such as ours. These solvers are part of their *Costly Global Optimization* (CGO) module which must be purchased separately from the base module already acquired (a demo is also available). Genetic algorithms could also be considered as an optimization engine; one interesting commercial option in this case is the Mathworks' *Genetic Algorithm and Direct Search Toolbox*.

2.3 Implementation of Custom Routines using Matlab

Since our objective was to build an automated design optimization tool, a suite of routines had to be implemented to provide the communication layer among the various third-party software tools embedded in this optimization framework. Matlab was chosen as the main platform for this optimization framework for two reasons. The first is its programmer interface, which provides the required flexibility. The second is the first author's experience using Matlab. The methods used and Matlab routines implemented are discussed in the following sections.

2.4 External Simulation Components

Two commercial software simulation tools were used as part of this optimization framework:

AKBOR2 (Kishk Consulting, Inc., U.S.A.) is used to model the antenna feed. It is a full-wave electromagnetic solver capable of modelling bodies of revolution made of conducting surfaces and several dielectric regions using the method of moments based on surface integral equations [1,9]. The main advantage of this solver as compared to 3-D solvers is its computational efficiency for the analysis of bodies of revolution. In addition, we only need to excite the fundamental single azimuthal mode ($m = 1$) and rotationally-symmetric structures do not couple distinct azimuthal modes. Therefore, the computational complexity of the simulations of interest is equivalent to that of a 2-D simulation.

Grasp, version 8 (TICRA Engineering Consultants, Denmark — www.ticra.com) is a commercial software program for the analysis of reflector antennas [2] based on physical optics. We use it to predict the far-field performance of the feed-reflector system as a whole.

3 Full-wave Simulation of Body-of-Revolution Antenna Feeds using the Method of Moments (AKBOR2)

AKBOR2 [1] is a full-wave solver for bodies of revolution comprised of multiple dielectric regions and conducting surfaces. It is based on the method of moments applied to boundary elements. A user license of the source code for this software tool was purchased from Kishk Consulting in October 2004. Version 6.01 was obtained, with the last change dating back to 28 July 1998, according to the comments in the source code. It is not clear, however, if any changes were implemented after this date.

3.1 Updates to Near-field Calculation Routines for Accurate Results

After a few months of testing with the original code, it was determined that the near fields provided by AKBOR2 were not sufficiently accurate to allow for proper determination of incident and reflected waves in a waveguide. Following discussions with Prof. Kishk regarding this matter, he sent us, in April 2005, an alternative, high-accuracy set of near-field calculation routines in replacement for those we had been using thus far. This has resolved the problem.

3.2 Improvements in Numerical Stability of AKBOR2

The AKBOR2 software, as delivered by Kishk Consulting, suffered some severe numerical instabilities. Several function evaluations performed as part of the computation of the matrix elements were implemented in a numerically unstable form. As a result, the matrix elements were, in some cases, severely affected by numerical noise. One of the clear manifestations of instability was that the computed matrix elements would differ based on the compiler platform and/or options used at compile time.

Such instabilities may not be too much of a concern for users who are manually crafting a limited number of antenna designs. In our case, it is very important to have a numerically stable algorithm since we are performing design optimizations requiring several thousand runs of the AKBOR2 code, which significantly increases the likelihood of triggering severe instabilities that could send the optimizer off course.

To address this issue, the unstable function evaluations were re-implemented in a numerically stable way. The theory and implementation of these changes are described in a separate document [10].

3.3 Dual-band Ku/X Feed Synthesis & Input File Generation for AKBOR2

To perform an electromagnetic simulation of the designed feed using AKBOR2, a compatible input file [1] is automatically generated based on the appropriate design parameters

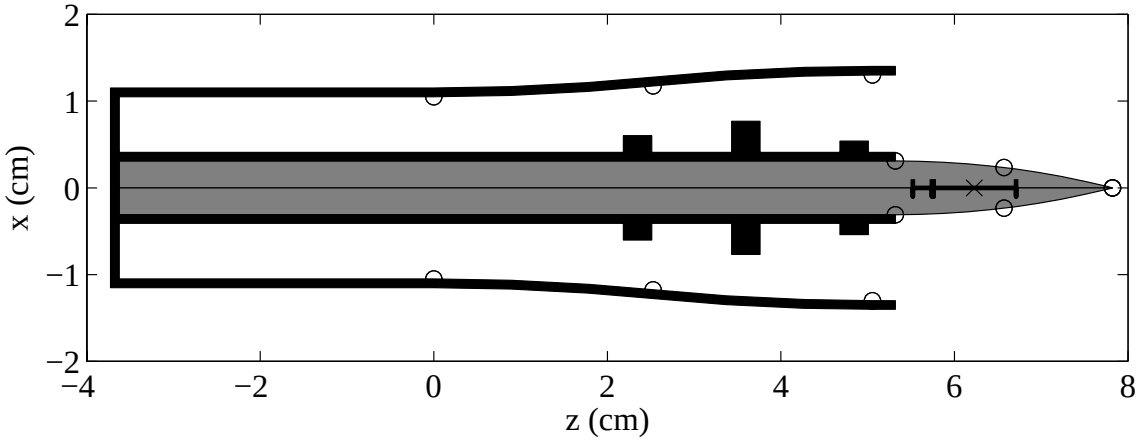

Figure 2: *Geometry of the dual-band Ku/X feed being optimized.*

applicable to the feed geometry under test. This file specifies the geometry and constitutive parameters, the excitation sources, and the desired diagnostic output.

Figure 2 illustrates the geometry applicable to our coaxial dual-band feed operating in the Ku and X bands. The Ku and X signals are guided along the circular and coaxial waveguides, respectively.

To improve the X-band coaxial aperture's radiation properties and impedance match to free space, it was decided to minimize the size of its internal conductor as much as possible [11] by filling the Ku-band circular waveguide with a high-constant dielectric material ($\epsilon_r = 9.8$) such as alumina. Starting from the opening of the circular waveguide, the dielectric cylinder is tapered down according to a two-section piecewise-quadratic profile. Both the profile and its slope are constrained to be monotonic. The resulting two variables control the length of the dielectric taper and its waist diameter.

To further improve the X-band coaxial aperture's impedance match, the coaxial waveguide flares out to a somewhat larger radius. The flare profile was devised to provide a fairly smooth transition, but its centre node was not included as part of the optimization variables to keep the problem to a reasonable complexity. The outer radius of the coaxial aperture was sized as large as possible without allowing for the propagation of TE/TM modes other than TE_{11}, in both the Ku and X bands (this is of course in addition to the TEM mode whose excitation must be avoided using proper excitation symmetry).

One of the main challenges in the design of a dual band Ku/X feed is to isolate the X-band channel from the Ku-band signal which tends to leak into the coaxial aperture. To block the Ku-band signal from entering the X-band channel, a low-pass filter was implemented inside the X-band coaxial channel using a series of three metallic rings, as can be seen in Figure 2. Figure 3 illustrates an equivalent circuit for this low-pass filter. Although our AKBOR2 simulations do not rely on this equivalent circuit, simulations using Ansoft HFSS have confirmed that the shunt capacitor is indeed a valid model for the coaxial metallic

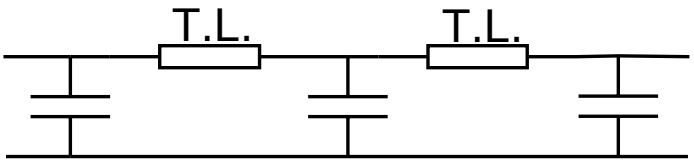

Figure 3: *Equivalent circuit for the 3-ring coaxial filter embedded in the coaxial waveguide.*

rings. The width of these rings was set to a fixed value, but the spacing and the individual ring thicknesses were optimized. The optimal element spacing for this filter is expected to correspond to less than half of the coaxial guided wavelength at some frequency within the Ku band.

In addition, to help improving the Ku-band input match, two "air gap rings" were placed inside the dielectric-filled circular waveguide. Optimal tuning of the position, width and depth of these rings was performed, allowing for a significant reduction of the reflection coefficient at Ku band. Details are given in section 6.2.

3.4 Simulation of Antenna Feed Using AKBOR2

The antenna feed is simulated using AKBOR2 independently from the reflector. Coarse parallelism was implemented by simultaneously running simulations at several frequencies over the bands of interest. In our dual-band example, simulations are performed at 9 frequency samples in each of the bands (Ku and X), for a total of 18 frequency samples. At Ku band, however, two simulations are required per frequency sample to extract the S-parameters since Ku-band frequencies propagate in both the circular and coaxial ports. Thus, a total of 27 frequency samples must be simulated, allowing to take full advantage of the available parallel-cpu capabilities. Simulations were performed on a dual-Xeon computer with hyper-threading capability, effectively providing four virtual processors with the equivalent processing power of somewhere between three and four Xeon processors.

3.5 S-Parameter Extraction from AKBOR2 Simulation Results

AKBOR2 has limited capability in terms of excitation sources. The only available sources are electric and magnetic dipoles. "Port" excitations, as typically available in other microwave simulation software packages, are not supported. Computing S-parameters thus required the implementation of in-house routines. The S-parameter extraction routines that were implemented support up to two ports in a given design. Circular-waveguide and coaxial-waveguide ports are supported. Note that all ports must support a single propagating mode.

3.5.1 Port excitation

To excite a given port, an x-oriented electric dipole is placed about one quarter of a wavelength away from a waveguide short within the port (see Figure 2 for coordinate system).

3.5.2 Wave Discrimination in Single-Moded Waveguide

The analysis of S-parameters requires the evaluation of the incoming and outgoing wave amplitudes in all of the single-moded waveguide ports. This is done in two parts:

1. First, the incoming and outgoing wave amplitudes are determined in terms of the x-component(see Figure 2) of the electric field along a reference longitudinal axis. In the case of a circular waveguide, the central axis is used ($r = 0$). In the case of a coaxial waveguide, the reference field axis is taken to be at a radius $r = (a + b))/2$, where a and b are the inner and outer radii of the coaxial waveguide, and at an azimuth angle $\theta = 0$ deg., that is, on the x axis.

   Based on the complex amplitudes of the x-component of the total electric field ($E_x(z)$) and the y-component of the total magnetic field ($H_y(z)$) measured at a position $z = z_0$ along the axis and away from perturbations, the amplitudes and phases of the x-component of the electric field of the incoming (travelling along $+z$) and outgoing (travelling along $-z$) waves at $z = 0$, E_{xA} and E_{xB}, are obtained as follows:

$$E_{xA} = \frac{E_x(z_0) + H_y(z_0)\frac{\eta_0}{\sqrt{\epsilon_r}\sqrt{1-(f_c/f)^2}}}{2\exp\left(-j\beta_z z_0\right)}; \tag{1}$$

$$E_{xB} = \frac{E_x(z_0) - H_y(z_0)\frac{\eta_0}{\sqrt{\epsilon_r}\sqrt{1-(f_c/f)^2}}}{2\exp\left(j\beta_z z_0\right)}, \tag{2}$$

   where η_0 is vacuum's intrinsic impedance, ϵ_r is the permittivity of the dielectric filling the waveguide, and f_c is the cutoff frequency of the waveguide mode. These equations apply to any TE wave in a homogeneous medium. We therefore use them for both the circular waveguide's TE_{11} mode and the coaxial waveguide's TE_{11} mode.

2. Second, the wave amplitudes are scaled so that a unit amplitude will correspond to a wave carrying 1 watt of power in the direction of propagation. The normalized incoming and outgoing wave amplitudes A and B are thus obtained from

$$A = E_{xA}/E_{xn} \tag{3}$$

$$B = E_{xB}/E_{xn}, \tag{4}$$

   where E_{xn} is the x component of the electric field of a unit-amplitude waveguide, measured on the longitudinal axis (the z-axis) defined above. It is calculated based on two different formulas for circular and coaxial waveguides, which we now describe.

   For the TE_{11} mode in circular waveguides, we use [12, §2, Eq. (29)]

$$E_{xn,circ.TE_{11}}(x = 0, y = 0) = \frac{15.849 \text{ volts}}{\epsilon_r^{1/4} a \left(1 - \left(f_{c,\mathrm{circTE}_{11}}/f\right)^2\right)^{1/4}}, \tag{5}$$

   where a is the waveguide radius, ϵ_r is the permittivity of the dielectric material filling the waveguide and

$$f_{c,\mathrm{circTE}_{11}} = c_0\sqrt{\epsilon_r}\frac{1.8412}{2\pi a} \tag{6}$$

is the cutoff frequency of a circular waveguide's TE_{11} mode.

For the TE_{11} mode in coaxial waveguides, a similar expression can be obtained by combining equations (43a) and (45) from [12] [3]:

$$E_{xn,coax.TE_{11}}\left(x=x_0,y=0\right)=\frac{Z_1\sqrt{\eta_0}\ \sqrt{\text{Watts}}}{\epsilon_r^{1/4}x_0\left(1-\left(f_{c,\text{coaxTE}_{11}}/f\right)^2\right)^{1/4}}$$

$$\text{with } Z_1\equiv\sqrt{\frac{\pi}{2}}\frac{\left(J_1\left(\chi'_{11}x_0/b\right)Y'_1\left(\chi'_{11}\right)-Y_1\left(\chi'_{11}x_0/b\right)J'_1\left(\chi'_{11}\right)\right)}{\sqrt{\left(\frac{J'_1(\chi'_{11})}{J'_1\left((a/b)\chi'_{11}\right)}\right)^2\left(1-\frac{1}{\left((a/b)\chi'_{11}\right)^2}\right)-\left(1-\frac{1}{\left(\chi'_{11}\right)^2}\right)}}. \quad (7)$$

Let us define some of the symbols used in the above expression:

- $x_0\equiv\frac{a+b}{2}$;
- the cutoff frequency of a coaxial waveguide's TE_{11} mode is given by

$$f_{c,\text{coaxTE}_{11}}=c_0\sqrt{\epsilon_r}\frac{\chi'_{11}\left(1+a/b\right)}{2\pi\left(a+b\right)}; \quad (8)$$

- a and b designate the outer and inner radii of the coaxial waveguide, respectively;
- J_1 and Y_1 are the first-order Bessel function of the first and second kinds, respectively;
- J'_1 and Y'_1 are the derivatives of J_1 and Y_1, respectively; and
- χ'_{11} is the first root of the equation

$$J'_1\left(\left(a/b\right)\chi'\right)Y'_1\left(\chi'\right)-Y'_1\left(\left(a/b\right)\chi'\right)J'_1\left(\chi'\right)=0, \quad (9)$$

  and is given in Table 2.4 from [12].

Note that these equations are in MKS units and the electric field is in units of V/m if a is in meters. These formulas were derived based on [12].

3.5.3 Single-port S-parameter Extraction

If the structure only features a single waveguide port or if only one of the ports supports a propagating mode at the frequency of operation, the input reflection coefficient S_{11} is simply calculated as $S_{11}=B/A$.

3.5.4 Two-port S-parameter Extraction

In the case where two waveguide ports support a propagating mode, computing the 2x2 S-parameter matrix can be performed using one of two techniques described in the following.

[3] We note that equation (45) from [12] must be corrected to $P=\frac{1}{\eta}\sqrt{1-\left(\frac{\lambda}{\lambda''_{ci}}\right)^2}\left|V''_i\right|^2$.

3.5.4.1 Two-port Analysis Using Reciprocity Principles

This technique consists of alternatively exciting each port in two separate AKBOR2 simulations, while shorting the other port. Let us denote as $(A_i)_k$ the incident complex amplitudes of the wave entering port i when port k is excited. Conversely, $(B_i)_k$ represents the reflected complex amplitude of the wave exiting port i when port k is excited. Using the incident and reflected wave amplitudes computed at both ports for both simulations, we can determine the 2-port S-parameter matrix elements by solving the following two complex systems of two equations in two unknowns:

$$\begin{bmatrix} (A_1)_1 & (A_2)_1 \\ (A_1)_2 & (A_2)_2 \end{bmatrix} \begin{bmatrix} S_{11} \\ S_{12} \end{bmatrix} = \begin{bmatrix} (B_1)_1 \\ (B_1)_2 \end{bmatrix}; \text{and} \tag{10}$$

$$\begin{bmatrix} (A_1)_1 & (A_2)_1 \\ (A_1)_2 & (A_2)_2 \end{bmatrix} \begin{bmatrix} S_{21} \\ S_{22} \end{bmatrix} = \begin{bmatrix} (B_2)_1 \\ (B_2)_2 \end{bmatrix}. \tag{11}$$

3.5.4.2 Two-port Analysis Using Matched-Port AKBOR2 Simulations

As an alternative, one could attempt to impedance match the port not being excited to prevent any reflections on that port. This is done by applying an impedance boundary condition equivalent to the mode's characteristic impedance on the end wall of the waveguide to be terminated.

Using this approach, the elements of the S-parameter matrix are determined in a more direct fashion. Exciting port #1 yields:

$$S_{11} = \frac{(B_1)_1}{(A_1)_1} \tag{12}$$

$$S_{21} = \frac{(B_2)_1}{(A_1)_1}, \tag{13}$$

while exciting port #2 yields:

$$S_{12} = \frac{(B_1)_2}{(A_2)_2} \tag{14}$$

$$S_{22} = \frac{(B_2)_2}{(A_2)_2}. \tag{15}$$

In cases where only S_{11} and S_{21} are desired for example, only one simulation is required (exciting port #1). This could be the case, for example, at a frequency which is normally meant to excite port #1 only.

Unfortunately, initial attempts to implement this technique using AKBOR2 have been unsuccessful. Prof. Kishk (the author of the code) has indicated that the reason for this problem is that the implementation of the surface impedance concept contains approximations only valid in the far field; it is therefore not accurate for near fields computations. The use of the matched-port technique would therefore require a near-field implementation of surface impedances in AKBOR2.

4 High-Frequency Simulation of Feed-Reflector System using Physical Optics

4.1 TICRA Grasp Commercial Simulator: Background Information

Electrically large reflectors can be modelled efficiently using the physical optics method [13]. As part of our antenna optimization framework, we use TICRA Grasp to model the electromagnetic scattering from large reflector antennas. In our dual-band feed design, we use a prime focus configuration with symmetric illumination. The main assumptions involved in using a high-frequency simulator such as TICRA Grasp are as follows for a symmetric design:

- No significant amount of power scatters back onto the antenna feed. If significant power were to be reflected back into the feed, that would affect the input mismatch coefficient of that feed and would not be accounted for. This assumption is valid, for example, in the case of a feed illuminating a sufficiently large reflector in a symmetric configuration, because the fraction of reflected power intercepting the feed is very small, being lower than the ratio of the cross sectional areas of the feed and reflector.
- The feed is located in the far-field of the reflector.
- The reflector is large with respect to the wavelength.

All the above assumptions are met in the case of the dual-band feed design being demonstrated here.

4.2 Reflector Simulation using Grasp

Grasp simulations are performed automatically using the command-line interface. The reflector's design parameters are automatically entered into the input file for Grasp by a specialized synthesis Matlab script. These parameters may be optimally (and automatically) chosen based on the feed far-field characteristic, or set to fixed values if retrofitting an existing reflector with a new multi-band feed, for example. The latter approach is used for our dual-band Ku/X feed design.

The feed used to illuminate the reflector is defined using Grasp's "tabulated feed" class. Specifying the co-polarization and cross-polarization patterns in both the E-plane and the H-plane is sufficient to completely characterize a body-of-revolution feed excited in the $m = 1$ azimuthal mode, since a rotationally-symmetric structure does not couple different azimuthal modes. Note that the $m = 1$ azimuthal mode can be excited, for example, using the TE_{11} mode in a circular or coaxial waveguide.

The effect of the change in position of the feed phase centre as a function of frequency is properly accounted for by changing the feed source position in the Grasp input file, consistent with the simulated frequency. In our dual-band Ku/X feed example, the feed was positioned such that its phase centre would coincide with the reflector's focal point at

the centre frequency of the Ku band. Thus, a degradation of the illumination's phase error occurs at other frequencies in the Ku band as well as in the X band. This degradation is accounted for in the simulations and reflects on the resulting aperture efficiency.

As described in Section 3.4 for the AKBOR2 simulations, coarse parallelism was implemented for Grasp simulations using concurrent runs at several frequencies over the bands of interest. In our dual-band Ku/X design, this implies performing 18 Grasp simulations to characterize a given feed design over 9 frequency points in both the Ku and X bands.

4.3 Extraction of Antenna Secondary Beam Performance Parameters

Since the simulation of the reflector is embedded in the feed optimization framework, the feed antenna's radiation performance can be evaluated directly from the characteristics of the secondary beam, rather than based on the feed far-field pattern (primary beam).

Three parameters are used to evaluate radiation performance:

Aperture Efficiency. This is the percentage efficiency of the complete feed-reflector system, relative to that of a uniform-amplitude, equiphase aperture with an area equivalent to the projected physical area of the reflector. Note that the simulations performed in this work do not account for ohmic losses.

Secondary-Beam Cross-Polarization Level. This is measured at a given scan angle range from boresight, corresponding to the tracking accuracy of the reflector antenna system. We have used 1 degree off-boresight for this purpose in the present work. This value corresponds approximately, in our design, to a 1-dB drop in directivity from the centre of the main beam. The cross-polarization level is defined as the relative power level of cross-polarized radiated fields with respect to co-polarized radiated fields in a given direction, and is given in dB.

Sidelobe Pattern Overshoot. This measures the maximum overshoot, in dB, over a given required antenna sidelobe envelope for scan angles beyond 1 degree, in any scan plane. In this work, we have enforced the following pattern in both the Ku and X bands over a range of scan angles going from $\theta = 1$ degree to $\theta = 30$ degrees off boresight:

$$G_{\text{req}} = \begin{cases} 29 - 25\log_{10}(\theta) \text{ dBi}, & 1.0^\circ \leq \theta < 20.0^\circ \\ -3.5 \text{ dBi}, & 20.0^\circ \leq \theta < 26.3^\circ \\ 32 - 25\log_{10}(\theta) \text{ dBi}, & \theta \geq 26.3^\circ \end{cases} \tag{16}$$

This pattern is based on the specification given in [14]. It is also found in the specification of many commercially-available reflector-antenna systems, such as a 2.4-meter multi-frequency reflector antenna sold by VertexRSI [15] (note that this model requires manually changing the RF feed on the assembly to switch from one band to another).

Three scan planes are sampled to measure the overshoot from the required pattern: the E-plane ($\phi = 0^\circ$), the H-plane($\phi = 90^\circ$) and the D-plane($\phi = 45^\circ$).

5 Definition of a Single-valued Scalar Cost Function

The global optimizer described in Section 2.2 relies on the definition of a single-valued scalar cost function which is minimized to identify the optimal set of design parameters.

Several sub-costs must generally be considered when designing an antenna. A list of the costs applicable to our dual-band Ku/X antenna feed design is first given in 5.1. These sub-costs must then be properly combined into a single-valued cost function that will be minimized. Various ways of accomplishing this are described in 5.2.

5.1 Description of Sub-costs Applicable to Dual-band Ku/X Feed

In our dual-band Ku/X feed design, there are six different performance sub-costs ($P_i,\ 1 \leq i \leq 6$) used in the objective cost analysis. They are:

- The S-parameters: $P_1 \equiv S_{11}(\text{Ku})$, $P_2 \equiv S_{22}(\text{X})$, $P_3 \equiv S_{21}(\text{Ku})$, all in dB;
- The aperture efficiency "cost", given in dB: $P_4 \equiv -A_{\text{eff,dB}} \equiv -10\log_{10}(A_{\text{eff}})$;
- The overshoot from the required sidelobe envelope, $P_5 \equiv max\{\text{Gain}(\theta,\phi) - \text{Required Gain Envelope}(\theta,\phi), \theta \leq 30^\circ\}$;
- The secondary-beam cross-polarization level, P_6 (in dB).

5.2 Combination of Sub-costs Into a Single Objective Cost

For each sub-cost P_i, let us define a target value, or goal, G_i, and a weight w_i. We seek a sensible optimization strategy that follows two important guidelines :

1. Giving priority to minimizing the sub-costs that are furthest above their corresponding target value; and
2. Individually minimizing each of the sub-costs to their lowest possible value.

Let us first consider the maximum cost approach, whereby the overall cost C is obtained by:

$$C = \max\left\{w_i \max(0, (P_i - G_i))\right\}, \qquad i = 1, ..., N. \tag{17}$$

The minimization of this max() function constitutes a *minimax* approach. Using this approach certainly satisfies the first guideline, because it only accounts for the largest weighted sub-cost. The drawback of this approach, however, is that if the goal G_i picked for sub-cost i turns out to be unrealistically low, then the optimization will stagnate upon reaching the lowest possible value for sub-cost i, i.e. the cost function cannot direct the optimizer to improve other sub-costs which may still have room for improvement.

Another approach consists of summing all weighted sub-costs:

$$C = \sum_{i=1}^{N} \left\{w_i \max(0, (P_i - G_i))\right\}. \tag{18}$$

Using this approach provides a much more continuous cost function. However, minimizing C may or may not correspond to a global minimization of all weighted sub-costs, because the reduction of certain sub-costs might come at the expense of the increase of some other ones, since only the summation is accounted for by the optimizer.

We found that an approach based on nonlinear cost summation could best satisfy both guidelines. The cost function

$$C = \left(\sum_{i=1}^{N} \max(0, \{w_i \left(P_i - G_i\right)\})^p \right)^{1/p} \tag{19}$$

in fact is a compromise between the maximum and summation approaches. Indeed, for $p = 1$, it is identical to the summation function, and as $p \to \infty$, it becomes identical to the maximum function. We found that a value $p = 2$ provides sufficient nonlinearity to not only account for all sub-costs at all times through the summation, but also to give priority to the highest sub-costs. We therefore can focus on the worst aspects of the antenna's performance, while avoiding stagnation when nearing the minimum achievable value for some of the large sub-costs.

6 Optimization of a Dual-band (Ku/X) Antenna Feed Aperture

A total of 12 control variables need to be optimized in our design, consistent with the description given in Section 3.3:

- 2 variables controlling the length and waist size of the profiled dielectric rod extending out of the circular waveguide and carrying the Ku-band signal;
- 3 variables controlling the heights of the three coaxial metallic rings forming the X-band filter;
- 1 variable controlling the spacing among the three coaxial metallic rings (note that two variables could have been used here, providing additional flexibility, but a single variable was used to keep to a reasonable number of variables);
- 2 variables controlling the heights of the two dielectric air gaps used for matching the input of the Ku-band channel;
- 2 variables controlling the positions of the two dielectric air gaps internal to the circular waveguide;
- 2 variables controlling the widths of the two dielectric air gaps.

To proceed efficiently, these variables were optimized in two independent stages. Because the two dielectric air gaps are internal to the circular waveguide, the 6 variables controlling them only significantly affect the Ku-band input match ($S_{11}(Ku)$) and cross-channel coupling

at Ku band ($S_{21}(Ku)$), and have no bearing on the X-band mismatch or on radiation characteristics. Therefore, we can optimize the feed in two separate stages: the first 6 variables are optimized in stage 1, and the last 6 variables are optimized in stage 2.

6.1 Stage-1 Optimization

The first six variables, controlling the dielectric profile and coaxial filter, were optimized using Tomlab's *glbfast* global optimizer using the nonlinear cost summation described in section 5.2 with a power $p = 2$. In performing this optimization, proper selection of the goal values for each parameter is crucial to steer the optimizer in the desired direction. The optimized results shown in Figure 4 were obtained based on the following goal values:

- Ku-band input mismatch (S_{11}): $G_1 = -12$ dB;
- X-band input mismatch (S_{22}): $G_2 = -20$ dB;
- Ku-band coupling (S_{21}): $G_3 = -20$ dB;
- Aperture Efficiency ($A_{\text{eff,dB}}$): $G_4 = -10\log_{10} 0.5 = 3.01$ dB, corresponding to an aperture efficiency of 50%;
- Overshoot from the required sidelobe pattern, $G_5 = 0$ dB;
- Secondary-beam cross-polarization level $G_6 = -35$ dB.

In this phase of the design, we were mainly concerned with issues associated with input mismatch and coupling, and have therefore favoured these criteria over the aperture efficiency in the goal selection. In future designs, we will likely require aperture efficiencies of at least 60% rather than 50%. The goal for the Ku-band mismatch was also modest in this stage of the optimization. The second stage of the optimization puts more focus on it.

All weights w_i (see Equation 17) were set to unity, except for the aperture efficiency (w_4) and sidelobe pattern overshoot (w_5) weights, which were set to 10, to ensure that the optimizer would not favour a solution with aperture efficiency lower than 50% or with any sidelobe overshoot.

Figure 4a shows the evolution of the cost function as a function of iterations. 1795 iterations were performed as part of this optimization, with each iteration taking approximately 1.4 minutes on a 3.2 GHz dual-cpu Xeon computer using both processors, for a total of just under 42 hours. Note that each iteration requires a total of 27 AKBOR2 simulations and 18 Grasp simulations, since for each of the 9 X-band frequency points the coaxial port must be excited, and for each of the 9 Ku-band frequency points both the circular and coaxial ports must be excited to extract the S-parameters. The resulting optimized design along with dimensions are shown in Figure 5, and the corresponding performance parameters as a function of frequency are shown in Figure 4b. The worst-case values for each cost parameter over the relevant frequency bands are displayed in Table 2.

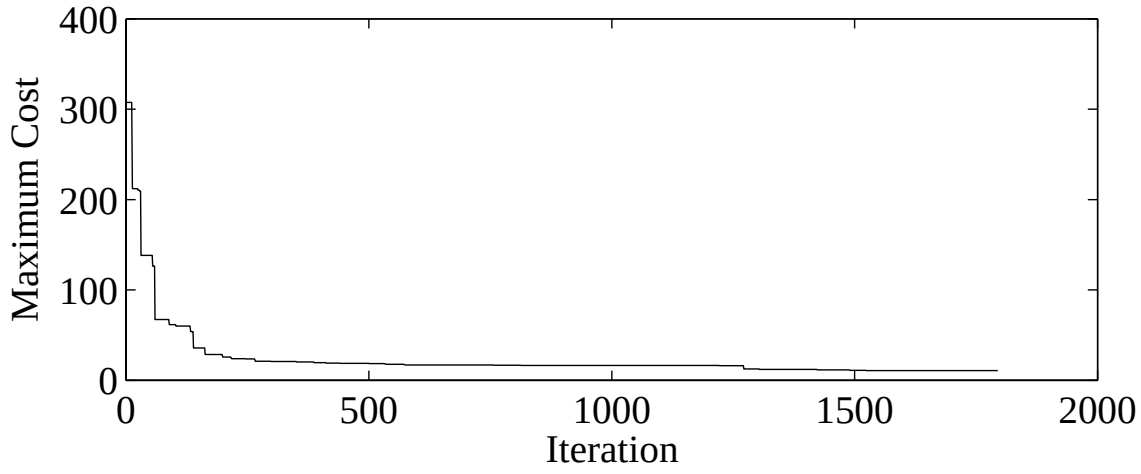

(a)

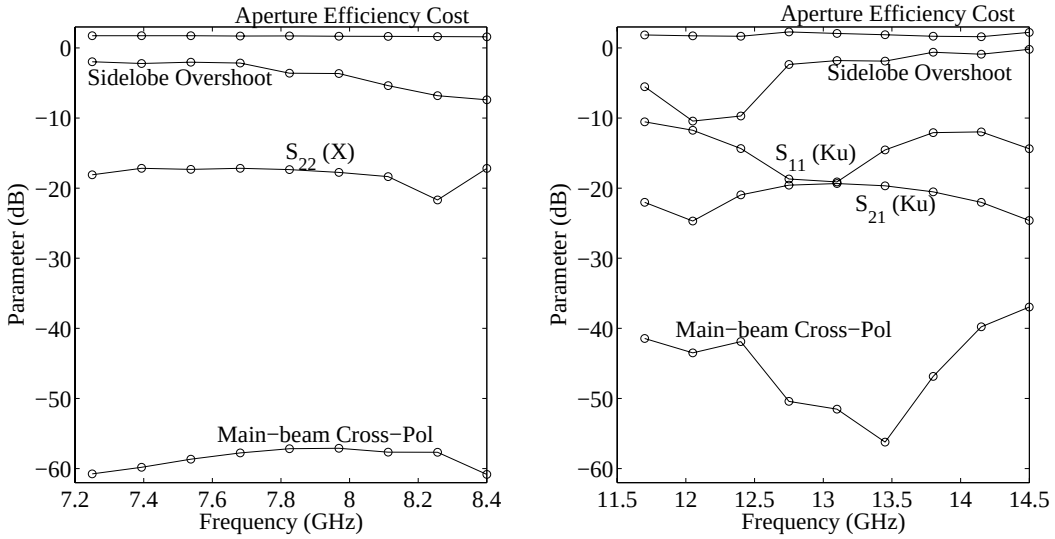

(b)

Figure 4: *Stage-1 optimization results (a) Graph of the overall cost as a function of the iteration number. (b) Plot of the various performance parameters of interest as a function of frequency in both the X band and Ku bands.*

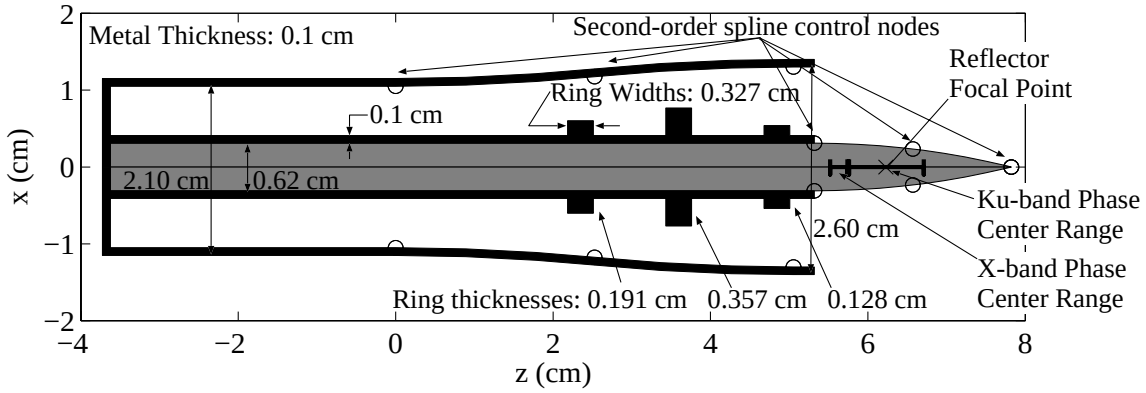

Figure 5: *Depiction of the stage-1 optimized feed design. Perfect conductor is shown in black, and dielectric material with* $\epsilon_r = 9.8$ *is shown in grey.*

	X band		**Ku band**	
Sub-cost Parameter	Stage-1	Stage-2	Stage-1	Stage-2
S_{11}			-10.5 **dB**	-16.2 **dB**
S_{22}	-17.2 dB	-17.0 dB		
S_{21}			-19.3 dB	-19.3 dB
Aperture Efficiency	67%	67%	59%	59%
Sidelobe Pattern Overshoot	-2.0 dB	-2.0 dB	-0.20 dB	-0.16 dB
Secondary-Beam Cross-Pol.	-57.1 dB	-56.8 dB	-37.0 dB	-36.8 dB

Table 2: *Worst-case performance parameters across both frequency bands. Results are given for both optimization stages. The main cost parameter affected by the second-stage optimization is* S_{11}.

Figures 6 through 9 illustrate the far-field patterns of the feed by itself and the feed-reflector combination, as obtained at the centre frequency of the Ku and X bands. The resulting radiation characteristics (aperture efficiency, sidelobe pattern overshoot, secondary-beam cross-polarization) are satisfactory, with aperture efficiency being well beyond the 50% goal that was set for the optimization, as can be seen in Table 2.

We note that further reductions of the cross-channel coupling (S_{21}) and X-band input mismatch, which are highly desirable, can likely be attained with the addition of a fourth and perhaps fifth metallic ring, which will increase the number of zeros in our lowpass coaxial filter.

6.2 Stage 2: Ku-band Input Mismatch Optimization Using Two Dielectric-Gap Rings

In this second optimization stage, two "air gap rings", shown in Figure 10, were added in the dielectric insert inside the circular waveguide. As Figure 11 illustrates, these gaps can be regarded as series inductances, although our simulations did not rely on this equivalent circuit. The optimizer only controlled these new internal rings, all other parameters being kept unchanged from the stage-1 optimization. These modifications only affect the Ku-band input mismatch, and do not interfere significantly with the radiation properties in either band or with the X-band input mismatch.

Figure 12a shows the evolution of the global cost during the second optimization. A total of 1458 iterations have been performed. The resulting optimized design is shown in Figure 10, in which the added Ku-band input matching circuit made out of two dielectric air gap rings is shown as an inset. Figure 12b shows the frequency-dependence of all subcosts of interest for this design. Table 2 shows that the only performance parameter that has undergone a significant change in the second-stage optimization is the Ku-band input mismatch, $S_{11}(Ku)$, which was reduced from -10.5 dB down to -16.2 dB.

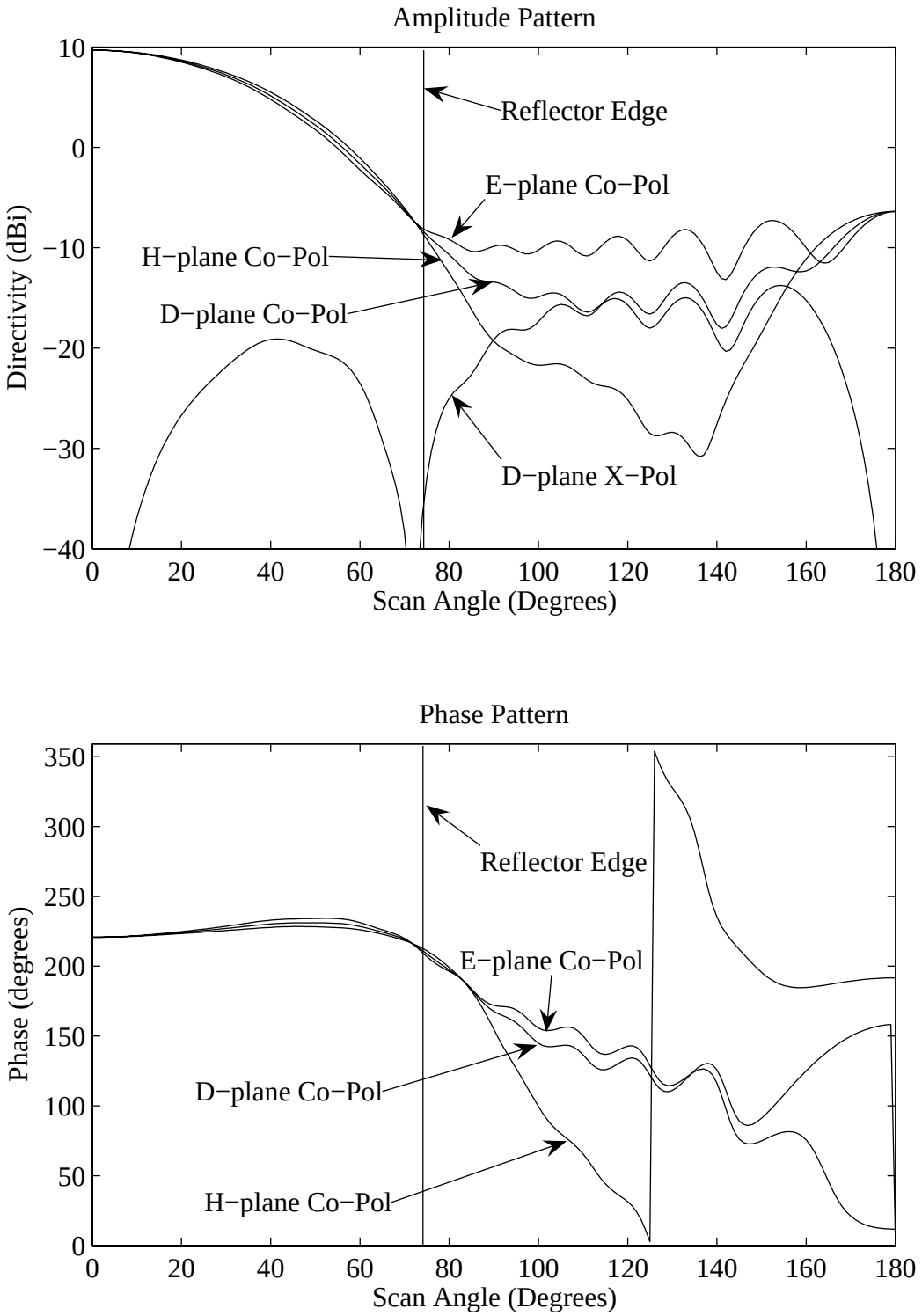

Figure 6: *Primary far-field amplitude and phase patterns in the centre of the Ku band (13.1 GHz), as obtained for the optimal feed design.*

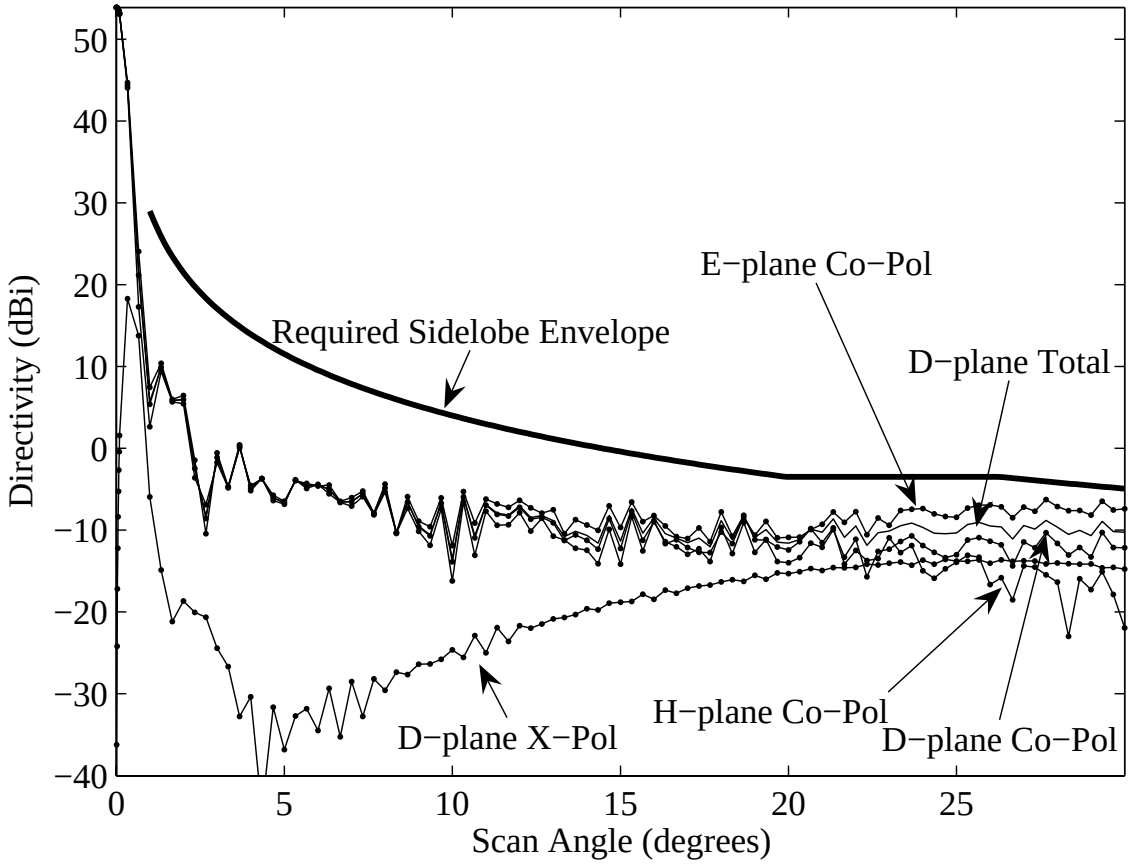

Figure 7: *Secondary far-field amplitude pattern in the centre of the Ku band (13.1 GHz), as obtained with the optimal feed design.*

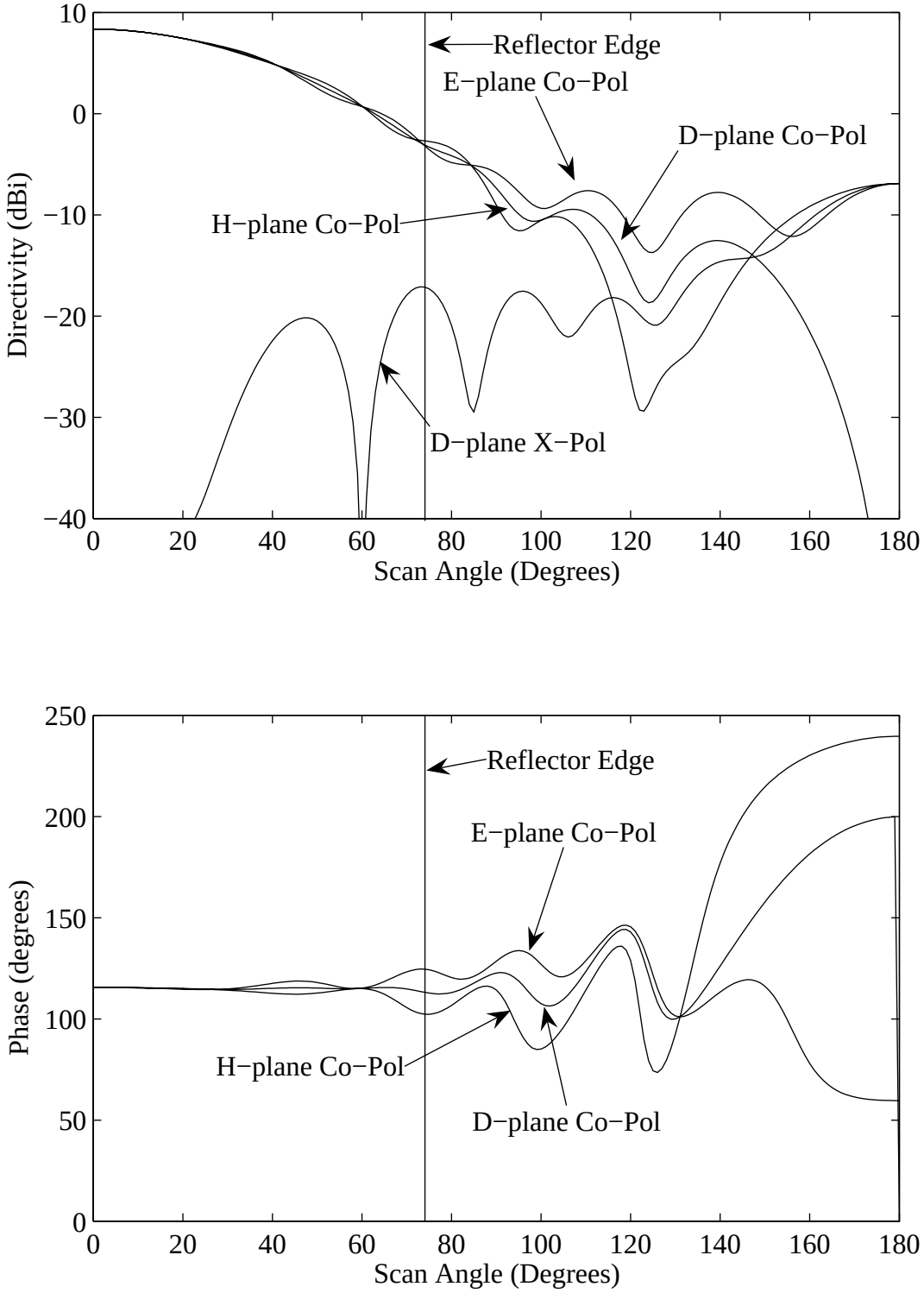

Figure 8: *Primary far-field amplitude and phase patterns in the centre of the X band (7.825 GHz), as obtained for the optimal feed design.*

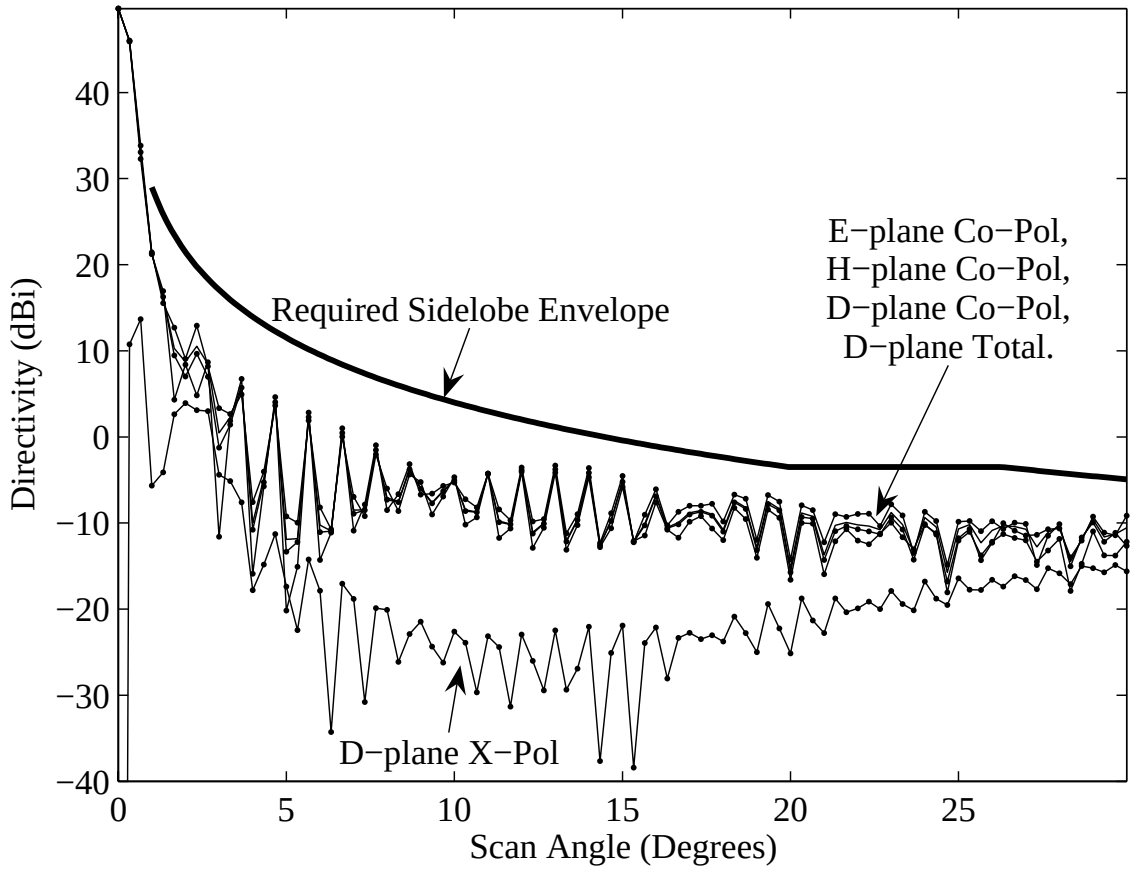

Figure 9: *Secondary far-field amplitude pattern in the centre of the X band (7.825 GHz), as obtained with the optimal feed design.*

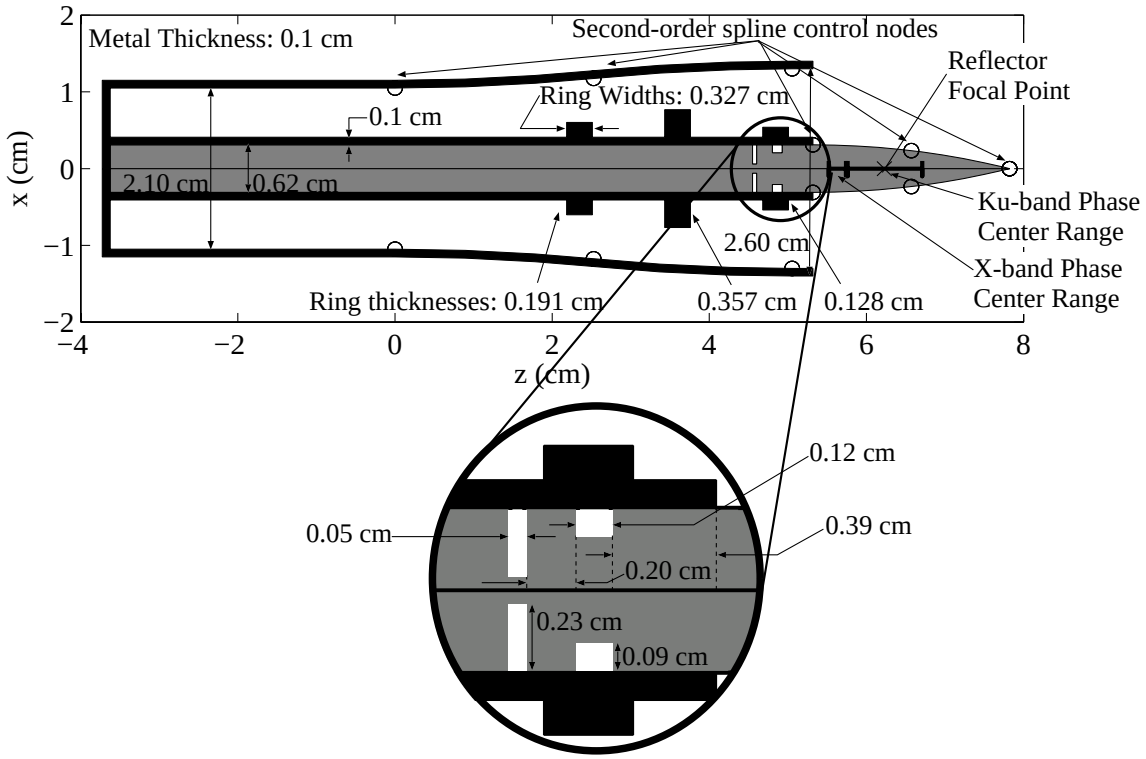

Figure 10: *Depiction of the second-stage optimized feed design together with an inset showing the two dielectric gap rings that were added to the Ku-band dielectric-filled circular waveguide ($\epsilon_r = 9.8$).*

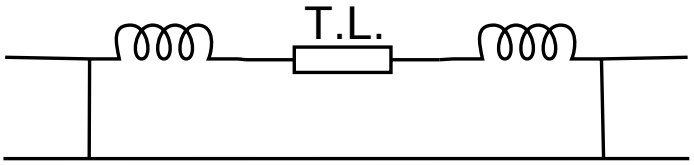

Figure 11: *Equivalent circuit for the 2 "air gap rings" embedded in the dielectric-filled circular waveguide.*

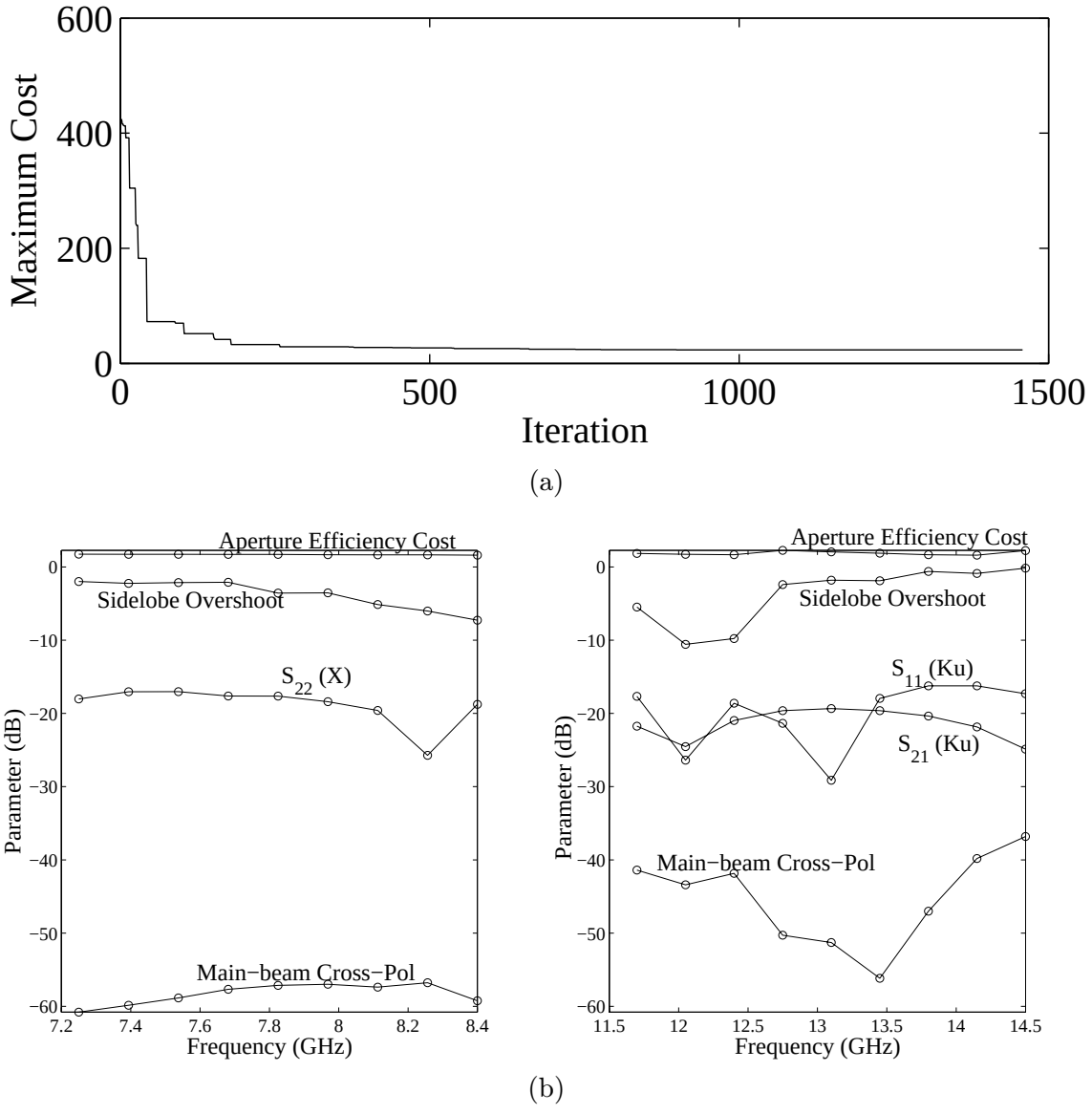

Figure 12: *Stage-2 optimization results (a) Graph of the overall cost as a function of iteration number. (b) Plot of the various performance parameters of interest as a function of frequency in both the X band and Ku bands.*

7 Conclusion

We have devised a new antenna design optimization framework, called FADO, suitable for body-of-revolution antenna feeds used in conjunction with reflectors. This new framework will allow for the efficient design of multi-band antenna feeds and other multi-band rotationally-symmetric antennas that are key to future communications platforms in software radios and possibly other multi-functional antennas in electronic warfare.

The design of the radiating stage of a compact dual-band Ku/X antenna feed for a symmetrically-fed single-reflector system was realized using this new design optimization framework. Radiation characteristics of the optimal design are satisfactory: 1) the resulting aperture efficiency is 67% at X band and 59% at Ku band; 2) the secondary-beam cross-polarization is better than -57 dB in the X band and better than -37 dB in the Ku band; and 3) the sidelobe pattern requirements are satisfied in both the X and Ku bands. A ring-based filter was shown to improve the coaxial rejection of the Ku-band signal (isolation of -19.3 dB) while providing adequate impedance matching capability for the X-band signal (input mismatch of -17 dB at X band). The addition of two air gap rings within the dielectric-filled circular waveguide allowed for an improvement of the Ku-band input mismatch from -10.5 dB to -16.2 dB.

Further improvements in the feed performance, particularly in regards to the isolation of the circular and coaxial waveguides at Ku band, may be obtained through the addition of more metallic rings within the coaxial waveguide. Possible improvements in the dielectric taper profile should also be investigated to help improving the isolation and Ku-band input impedance match.

Straightforward extensions of the design framework shown here could allow for the synthesis and optimization of dual-reflector, and/or offset-fed antenna systems. In addition, FADO may be extended for use with other antenna simulation tools, allowing to address other classes of antenna geometries which may not be rotationally symmetric.

We note that other ongoing research efforts at DRDC Ottawa and the CRC are focusing on the development of the other feed components, which connect upstream of the radiating stage. These include polarizers, orthomode transducers, and coaxial waveguide couplers.

References

[1] Kishk, Ahmed A. (2001), Scattering and radiation from multi homogeneous dielectric regions partially coating conducting surfaces using method of moments bodies of revolution (AKBOR2), Kishk Consulting, Inc., Oxford, Mississipi.

[2] (2000), Grasp 8 software user manual, 8.2.0 ed, TICRA Engineering Consultants, Copenhagen, Denmark.

[3] Telesat satellite channel frequencies (Online), `http://www.telesat.ca/satellites/frequencies/index.htm` (Access Date: 21 November 2005).

[4] Clénet, Michel (2005), Satcom specifications for SDR front-end terminal, (DRDC Ottawa TN 2005-117), Defence R&D Canada – Ottawa. Internal publication.

[5] Kerr, Peter, Jeffs, Allan, Davis, Ian, Granet, Christophe, Forsyth, Ross, and Clarke, Nick (2004), Multi-band satellite communications terminals for land communications, In *Proceedings of the Land Warfare Conference 2004*, pp. 167–172, Melbourne.

[6] The Mathworks — Matlab and Simulink for technical computing (Online), `http://www.mathworks.com` (Access Date: 24 November 2005).

[7] Matlab Optimization — Tomlab (Online), `http://tomlab.biz` (Access Date: 21 November 2005).

[8] Jones, D.R., Perttunen, C.D., and Stuckman, B.E. (1992), Global optimization: beyond the Lipschitzian model, In *Proceedings of the 1992 IEEE International Conference on Systems, Man and Cybernetics*, Vol. 1, pp. 566–570.

[9] Kishk, A. A. (1986), Different formulations for numerical solution of single or multibodies of revolution with mixed boundary conditions, *IEEE Transactions on Antennas and Propagation*, 34(5), 666–673.

[10] Choinière, Éric (2005), Numerical stabilization of AKBOR2, a body-of-revolution electromagnetic solver — Identification of unstable routines and Fortran implementation of stable replacement routines, (DRDC Ottawa TN 2005-195), Defence R&D Canada – Ottawa. Internal publication.

[11] Bird, Trevor S., James, Graeme L., and Skinner, Stephen J. (1986), Input mismatch of TE_{11} mode coaxial waveguide feeds, *IEEE Transactions on Antennas and Propagation*, 34(8), 1030–1033.

[12] Marcuvitz, N. (1986), Waveguide handbook, Peter Peregrinus Ltd.

[13] Balanis, Constantine A. (1989), Advanced electromagnetics, John Wiley & Sons, Inc.

[14] Intelsat (2002), Standards C, E and K, Antenna and wideband RF performance characteristics of Ku-band earth stations accessing the Intelsat space segment for standard services, (Technical Report IESS 208), Intelsat.

[15] Model 2.4-meter SF-LT C,X,Ku and Ka-band motorized flyaway (Online), `http://www.tripointglobal.com/Antennas/Data0.pdf` (Access Date: 21 November 2005). Specification sheet by VertexRSI, a TriPoint Global Company.

DOCUMENT CONTROL DATA

(Security classification of title, body of abstract and indexing annotation must be entered when document is classified)

1. ORIGINATOR (the name and address of the organization preparing the document. Organizations for whom the document was prepared, e.g. Centre sponsoring a contractor's report, or tasking agency, are entered in section 8.)

Defence R&D Canada – Ottawa
3701 Carling Avenue, Ottawa, Ontario, Canada K1A 0Z4

2. SECURITY CLASSIFICATION (overall security classification of the document including special warning terms if applicable).

UNCLASSIFIED

3. TITLE (the complete document title as indicated on the title page. Its classification should be indicated by the appropriate abbreviation (S,C,R or U) in parentheses after the title).

A design optimization framework for multi-band body-of-revolution antenna feeds: Application to a prime-focus dual-band Ku/X coaxial feed

4. AUTHORS (last name, first name, middle initial)

Choinière, Éric ; Morin, Gilbert A.

5. DATE OF PUBLICATION (month and year of publication of document)

December 2005

6a. NO. OF PAGES (total containing information. Include Annexes, Appendices, etc).

38

6b. NO. OF REFS (total cited in document)

15

7. DESCRIPTIVE NOTES (the category of the document, e.g. technical report, technical note or memorandum. If appropriate, enter the type of report, e.g. interim, progress, summary, annual or final. Give the inclusive dates when a specific reporting period is covered).

Technical Memorandum

8. SPONSORING ACTIVITY (the name of the department project office or laboratory sponsoring the research and development. Include address).

Defence R&D Canada – Ottawa
3701 Carling Avenue, Ottawa, Ontario, Canada K1A 0Z4

9a. PROJECT NO. (the applicable research and development project number under which the document was written. Specify whether project).

15CX01

9b. GRANT OR CONTRACT NO. (if appropriate, the applicable number under which the document was written).

10a. ORIGINATOR'S DOCUMENT NUMBER (the official document number by which the document is identified by the originating activity. This number must be unique.)

DRDC Ottawa TM 2005-216

10b. OTHER DOCUMENT NOs. (Any other numbers which may be assigned this document either by the originator or by the sponsor.)

11. DOCUMENT AVAILABILITY (any limitations on further dissemination of the document, other than those imposed by security classification)

(X) Unlimited distribution
( ) Defence departments and defence contractors; further distribution only as approved
( ) Defence departments and Canadian defence contractors; further distribution only as approved
( ) Government departments and agencies; further distribution only as approved
( ) Defence departments; further distribution only as approved
( ) Other (please specify):

12. DOCUMENT ANNOUNCEMENT (any limitation to the bibliographic announcement of this document. This will normally correspond to the Document Availability (11). However, where further distribution beyond the audience specified in (11) is possible, a wider announcement audience may be selected).

13. ABSTRACT (a brief and factual summary of the document. It may also appear elsewhere in the body of the document itself. It is highly desirable that the abstract of classified documents be unclassified. Each paragraph of the abstract shall begin with an indication of the security classification of the information in the paragraph (unless the document itself is unclassified) represented as (S), (C), (R), or (U). It is not necessary to include here abstracts in both official languages unless the text is bilingual).

The development of software radios has brought about a need for multi-band antenna feeds for use in the radio-frequency front-ends of satellite ground terminals. To provide the tools necessary for the design of such feeds, we have developed the *Framework for Antenna Design and Optimization* (FADO), a computer-based antenna design optimization framework based on the combination of custom-designed synthesis and analysis software, a commercial body-of-revolution electromagnetics simulation tool (AKBOR2, by Kishk Consulting), a high-frequency reflector modelling tool (Grasp, by TICRA), and a global optimizer (*glbfast*, part of the Tomlab optimization suite). The capabilities of this new design tool are demonstrated through the design of a compact dual-band Ku/X coaxial antenna feed for a 4.6-m single-reflector antenna.

A compact dual-band feed was designed by combining a dielectric-filled circular waveguide ending in a tapered dielectric rod, which launches the Ku-band waves, and a coaxial aperture launching the X-band waves. The use of a high dielectric constant material ($\epsilon_r = 9.8$) within the Ku-band's circular waveguide resulted in a fairly compact dual-band feed design aperture with an outer diameter of 2.8 cm.

Directly integrating both the feed scattering parameters and the secondary beam characteristics within a global optimization loop, this dual-band Ku/X coaxial antenna feed was designed and optimized using FADO. Proper reflector illumination was achieved in both frequency bands. This resulted in aperture efficiencies above 67% at X band and 59% at Ku band, secondary-beam cross-polarization levels of -57 dB at X band and -37 dB at Ku band, and sidelobe levels lower than the maximum sidelobe envelope per IntelSat's standard. A ring-based filter integrated in the coaxial channel is shown to improve coaxial rejection of the Ku-band signal while providing adequate impedance matching capability for the X-band signal. A Ku-band isolation better than -19.3 dB and an X-band input mismatch better than -17 dB are achieved. Further improvements in the channel isolation may be achieved using additional coaxial rings in the coaxial waveguide.

As part of a separate optimization, two air gap rings were integrated within the dielectric-filled circular waveguide, which allowed for an improvement of the Ku-band input mismatch from -10.5 dB to -16.2 dB.

The capabilities of FADO will allow for the efficient synthesis and optimization of multi-band antenna feeds integrated in symmetrically-fed single reflector antennas. In addition, straightforward extensions of the design framework could allow for the synthesis and optimization of dual-reflector, and/or offset-fed antenna systems. Finally, FADO may be extended for use with other antenna simulation tools, to address other classes of antenna geometries which may not be rotationally symmetric.

14. KEYWORDS, DESCRIPTORS or IDENTIFIERS (technically meaningful terms or short phrases that characterize a document and could be helpful in cataloguing the document. They should be selected so that no security classification is required. Identifiers, such as equipment model designation, trade name, military project code name, geographic location may also be included. If possible keywords should be selected from a published thesaurus. e.g. Thesaurus of Engineering and Scientific Terms (TEST) and that thesaurus-identified. If it not possible to select indexing terms which are Unclassified, the classification of each should be indicated as with the title).

Multi-band antennas;Body of revolution;Design optimization;Satellite Ground Terminal; Antenna feed;Global optimization

Defence R&D Canada

Canada's leader in Defence
and National Security
Science and Technology

R & D pour la défense Canada

Chef de file au Canada en matière
de science et de technologie pour
la défense et la sécurité nationale

www.drdc-rddc.gc.ca